ARMY RESEARCH LABORATORY

Microstructures and Mechanical Responses of Powder Metallurgy Noncombustive Magnesium Extruded Alloy by Rapid Solidification Process in Mass Production

by Katsuyoshi Kondoh, EL-Sayed Ayman Hamada, Hisashi Imai, and Junko Umeda

ARL-CR-647 **May 2010**

prepared by

Joining and Welding Research Institute
Osaka University
11-1 Mihogaoka
Ibaragi, Osaka, 567-0047, Japan

under contract

FA-5209-09-P-0158

NOTICES

Disclaimers

The findings in this report are not to be construed as an official Department of the Army position unless so designated by other authorized documents.

Citation of manufacturer's or trade names does not constitute an official endorsement or approval of the use thereof.

Destroy this report when it is no longer needed. Do not return it to the originator.

Army Research Laboratory
Aberdeen Proving Ground, MD 21005-5066

ARL-CR-647 **May 2010**

Microstructures and Mechanical Responses of Powder Metallurgy Noncombustive Magnesium Extruded Alloy by Rapid Solidification Process in Mass Production

Katsuyoshi Kondoh, EL-Sayed Ayman Hamada, Hisashi Imai, and Junko Umeda
Joining and Welding Research Institute

prepared by

Joining and Welding Research Institute
Osaka University
11-1 Mihogaoka
Ibaragi, Osaka, 567-0047, Japan

under contract

FA-5209-09-P-0158

REPORT DOCUMENTATION PAGE	Form Approved OMB No. 0704-0188

1. REPORT DATE *(DD-MM-YYYY)*	2. REPORT TYPE	3. DATES COVERED (From - To)
May 2010	Final	December 2008–Present

4. TITLE AND SUBTITLE
Microstructures and Mechanical Responses of Powder Metallurgy Noncombustive Magnesium Extruded Alloy by Rapid Solidification Process in Mass Production

5a. CONTRACT NUMBER
FA-5209-09-P-0158

5b. GRANT NUMBER

5c. PROGRAM ELEMENT NUMBER

6. AUTHOR(S)
Katsuyoshi Kondoh, EL-Sayed Ayman Hamada, Hisashi Imai, and Junko Umeda

5d. PROJECT NUMBER
1L162618AH80

5e. TASK NUMBER

5f. WORK UNIT NUMBER

7. PERFORMING ORGANIZATION NAME(S) AND ADDRESS(ES)
Joining and Welding Research Institute
Osaka University
11-1 Mihogaoka
Ibaragi, Osaka, 567-0047, Japan

8. PERFORMING ORGANIZATION REPORT NUMBER

9. SPONSORING/MONITORING AGENCY NAME(S) AND ADDRESS(ES)
U.S. Army Research Laboratory
ATTN: RDRL-WMP-E
Aberdeen Proving Ground, MD 21005-5066

10. SPONSOR/MONITOR'S ACRONYM(S)

11. SPONSOR/MONITOR'S REPORT NUMBER(S)
ARL-CR-647

12. DISTRIBUTION/AVAILABILITY STATEMENT
Approved for public release; distribution is unlimited.

13. SUPPLEMENTARY NOTES

14. ABSTRACT
Spinning water atomization process (SWAP), one of the rapid solidification processes, promised to produce coarse noncombustible magnesium alloy powder 1–4 mm long and have fine α-Mg grains and Al2Ca intermetallic compounds. SWAP had economical and safe benefits in producing coarse Mg alloy powders with very fine microstructures in the mass production process due to its extreme high solidification rate compared to the conventional atomization process. AMX602 (Mg-6%Al-0.5%Mn-2%Ca) powders were compacted at room temperature. Their green compacts, with a relative density of about 85%, were heated at 573–673 K for 300 s in Ar gas atmosphere and immediately consolidated by hot extrusion. Microstructure observation and evaluation of mechanical properties of the extruded AMX602 alloys were carried out. The uniform and fine microstructures, with grains <0.45–0.8 μm via dynamic recrystallization during hot extrusion, were observed and much smaller in comparison to the extruded AMX602 alloy fabricated from cast ingot. The extremely fine intermetallic compounds, 200–500 nm in diameter, were uniformly distributed in the matrix of powder metallurgy extruded alloys. These microstructures caused excellent mechanical properties of the wrought alloys. For example, in the case of AMX602 alloys extruded at 573 K, tensile strength of 447 MPa, yield stress of 425 MPa, and 9.6% elongation were obtained.

15. SUBJECT TERMS
rapid solidification, noncombustive magnesium alloy, powder, hot extrusion, water atomization, AMX602, mechanical response, microstructure

16. SECURITY CLASSIFICATION OF:			17. LIMITATION OF ABSTRACT	18. NUMBER OF PAGES	19a. NAME OF RESPONSIBLE PERSON
a. REPORT	b. ABSTRACT	c. THIS PAGE			Tyrone Jones
Unclassified	Unclassified	Unclassified	UU	26	19b. TELEPHONE NUMBER (*Include area code*) 410-278-6223

Standard Form 298 (Rev. 8/98)
Prescribed by ANSI Std. Z39.18

Contents

List of Figures

List of Tables

Acknowledgments

I would like to thank Mr. Tyrone Jones of the U.S. Army Research Laboratory for the technical vision and collaboration in this international program. Mr. Jones initiated this successful program through the International Technology Center - Pacific (ITC-PAC) and set technical key performance parameters that have led to the development of a high-strength, high-ductility lightweight magnesium alloy for applied structural applications. I would also like to thank Dr. Jitendra Singh of ITC-PAC for his drafting and management of this research contract.

1. Introduction

Magnesium has a low density of 1.8 kg/m^3, and its alloy is lightest of the industrial metals. It has a higher specific tensile strength than other metals, such as aluminum, iron, and titanium alloys (*1*). Therefore, it promises to save energy and reduce air pollutants, such as CO_2, SO_x, and NO_x, through weight reduction as structural components used in automobiles, motorcycles, and airplanes. In general, the strengthening of materials is useful for the weight reduction of their components. Grain refinement is one of the effectively strengthening processes. For example, the Hall-Petch equation is well known to quantitatively express the effect of the grain size on the yield stress of the materials (*2*). In this equation, a larger Hall-Petch constant, corresponding to its gradient of the equation, is more effective to increase the strengthening effect. When comparing the constant of magnesium and aluminum, the former is about twice as large as the latter (*3*). Accordingly, the grain refinement process is often employed to improve the mechanical properties of magnesium alloys. For example, hot extrusion, rolling, forging, high-pressure torsion, accumulative roll bonding, and roll compaction, which are typical severe plastic working processes, are useful to refine grains of the matrix via dynamic recrystallization (*4–8*). Strong texture, however, is formed in the matrix at the same time these plastic working processes are applied to the magnesium alloys. It is concluded that the severe plastic deformation is available to increase the tensile property by grain refinement but causes anisotropy in the magnesium alloys (*9*).

On the other hand, a rapid solidification process is useful to prepare ultrafine microstructures of metal powders, such as iron, aluminum, magnesium, copper, and their alloys (*10–13*). Nonequilibrium phases and amorphous and metallic glass structures can be also built up in the rapidly solidified metal powders (*14–16*). They also promise to improve the mechanical and physical properties of their consolidated materials. In general, microstructure refinement by the rapid solidification process strongly depends on the particle size. For example, the finer powders are significantly more effective in forming smaller grain size. It is obvious, however, that finer powders of active metals, such as aluminum, magnesium, and titanium, are very dangerous to handle. It is also difficult to consolidate them via the solid-state sintering process because of their thermally stable oxide films covering the powder surfaces. Therefore, from the previous two points of view, it is necessary to handle and consolidate the fine magnesium powders, ribbons, and flakes under a vacuum condition.

In this study, the microstructure observation and structural analysis were carried out on 1–4-mm-long coarse magnesium powders prepared by spinning water atomization process (SWAP). This process has already been commercialized to produce stainless steel fine particles and high-strength aluminum alloy powders. The noncombustive magnesium alloy (*17*) AMX602 (Mg-6%Al-0.5%Mn-2%Ca) was selected for the matrix alloy. While consolidating AMX602

powders by hot extrusion, the effect of the temperature in the preheating process before extrusion on the microstructural and mechanical properties of the extruded AMX602 powder metallurgy (P/M) alloys was investigated in detail. The extruded material fabricated using AMX602 cast ingot was employed as the reference. P/M AMX602 alloys showed extremely fine grains with a diameter of 0.45–0.8 μm, a good balance of tensile strength with 422 MPa, and 14.2% elongation at room temperature.

2. Experimental

2.1 Raw Materials

In SWAP powder preparation, illustrated in figure 1a, the noncombustive AMX602 magnesium alloy ingot was melted at 1053 K in the ceramic crucible. A protective layer of inert gas surrounded the ingot during the melting phase of SWAP preparation. The molten metals were directly streamed into the spinning water from the crucible nozzle. Table 1 shows chemical compositions of AMX602 alloy powders prepared by SWAP. The required calcium content of 2.09% was satisfied. The impurity content of Fe and Cu was successfully controlled to less than 0.005% because they are corrosive elements against magnesium alloys. As shown in figure 1b, the coarse AMX602 powders are 1–4 mm long and have an irregular shape. The cast ingot with the same composition was also prepared as a reference input material.

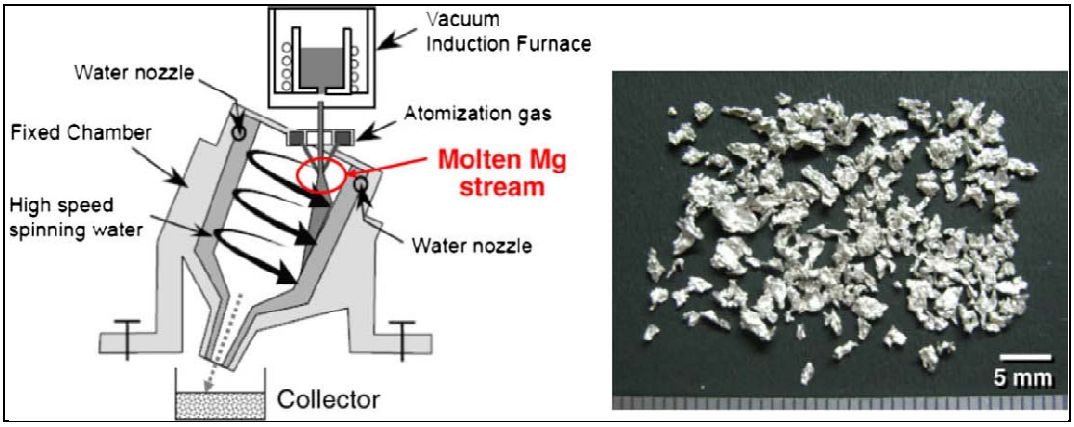

Figure 1. (a) Illustration of SWAP equipment to produce rapidly solidified Mg alloy powders and (b) morphology of coarse noncombustive magnesium alloy powder (AMX602 prepared by SWAP).

Table 1. Chemical compositions of noncombustive magnesium alloy powders.

Al	Zn	Mn	Fe	Si	Cu	Ca	Mg
6.01	0.007	0.26	0.002	0.038	0.004	2.09	Balance

2.2 Powder Consolidation

The powder was consolidated at room temperature by using a 2000-kN hydraulic press machine to fabricate the green compact, which had a relative density of 85% and a diameter of 42 mm. The columnar compact and cast ingot were heated at 573–673 K for 180 s in an argon gas atmosphere and immediately consolidated into full density by hot extrusion. The extrusion ratio of 37 and 1-m/s extrusion speed were used in this study.

2.3 Evaluation

To evaluate the thermal stability of the microstructures of raw powders, the differential thermal analysis (DTA, Shimadzu DTG-60) and x-ray diffraction (XRD, Shimadzu XRD-6100) analysis were carried out. An optical microscope (Olympus, BX-51P) and a scanning electron microscope (SEM, JOEL JSM-6500F) with energy-dispersed x-ray spectrometer (EDS, JOEL EX-64175JMU) were used to investigate the grain size and intermetallic compounds of the raw powders and their extruded alloys. The image-scanning software (Image Pro-Plus II) was applied to the photos to estimate the grain size distribution. The micro-Vicker's hardness of powders and wrought materials was measured by using the hardness tester (Shimadzu HMV-2T). The tensile test specimens were machined from the extruded alloys and evaluated at room temperature under a strain rate of $5*10^{-4}$/s. The fractured surfaces of the tensile test specimens were observed by SEM to investigate the fracturing mechanism of the magnesium alloys.

3. Results and Discussion

Figure 2 shows SWAP-prepared optical microstructures of AMX602 cast ingot (figure 2a), as-received fine powders <0.5 mm (figure 2b), and coarse powders over 1 mm (figure 2c). The cast ingot material consists of coarse α-Mg grains 60–150 μm in diameter, and some intermetallic compounds are observed at their grain boundaries. As shown in (figure 2b), fine powders reveal small dendrite structures formed during the rapid solidification of molten Mg alloy droplets after atomization. A mean dendrite arm spacing (DAS) of fine powders (figure 2b) is 0.97 μm. The coarse powders shown in figure 2c indicate large grains 4–8 μm in diameter caused by a reduced solidification rate during atomization. The grain mean size is 6.7 μm. According to the following equation (*18*), the DAS value suggests the estimated solidification rate (R) of the fine AMX602 powders.

$$\lambda = 35.5R^{-0.31} \qquad \lambda : \text{DAS}(\mu\text{m}),\ \text{R} : \text{Solidification rate (K/s)} \qquad (1)$$

As a result, the solidification rate of fine and coarse Mg alloy powders via SWAP is 1.1×10^5 K/s and 6.8×10^3 K/s, respectively. The mean particle size of fine and coarse powders via SWAP is 0.36 and 1.87 mm, respectively. They are much larger than the other alloy powders (100–200 μm) via the conventional atomization process. This indicates that SWAP Mg alloy

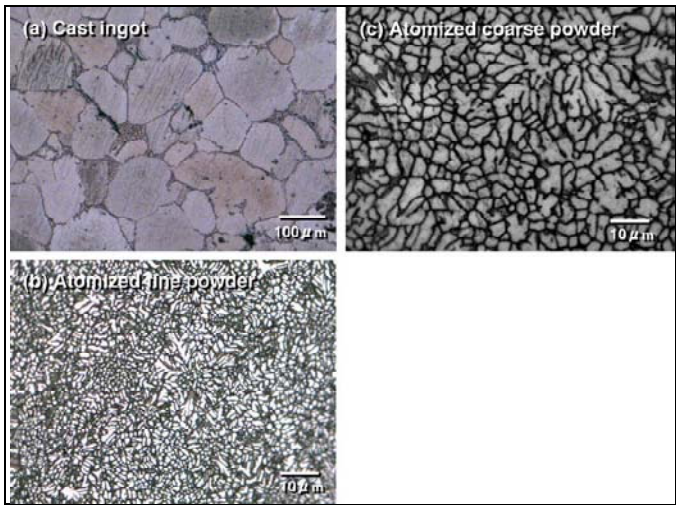

Figure 2. Optical microstructures of input raw materials: (a) as-cast ingot billet, (b) as-received fine SWAP powder, and (c) coarse powder.

powders are safe to handle and show very fine microstructures due to high solidification rare as mentioned above. Therefore, SWAP has an economical benefit when applied to the mass production process of powder metallurgy Mg alloys. On the other hand, the cast AMX602 alloy had a very small solidification rate of 0.6 K/s, calculated by the previous equation, which was equal to that of the conventional cast Mg alloys (*19*). Furthermore, no intermetallic compounds were detected at the grain boundaries in either powder due to very high rapid solidification rate.

Figure 3 shows DTA profiles of the atomized coarse powders and cast ingot. The extremely large exothermic peaks detected at 723 K in both profiles are caused by changing the heating rate from 10 to 5 K/min. The large endothermic peaks are detected at 798–800 K in both and correspond to a melting point of Al_2Ca intermetallics (*17*). The endothermic peak at about 880 K is due to the appearance of a liquid phase of this alloy. According to these results, the extrusion temperature of the atomized powders and cast ingot should be controlled to less than melting point of Al_2Ca intermetallics at 798 K. In this study, the preheating temperature of the green compact and cast ingot material is set at 573–673 K.

Figure 4 shows XRD patterns of the input raw material and its extruded alloys at 573 and 673 K. In the case of SWAP powders shown in figure 4a, the magnesium oxide (MgO) peak is detected at $2\theta=43°$, which is caused by oxidation of molten Mg alloy droplets during water atomization. MgO films covering the powder surfaces are thermally stable. However, it is easy to break them by applying a very low pressure in consolidation because of their porous structures (*20*). No Al_2Ca intermetallic peak is shown in the profile of the raw powder, but it is detected in the extruded alloys. This means that Al and Ca are solid-soluted in the matrix of the as-received raw powder by rapid solidification. However, Al_2Ca compounds are precipitated due to the elevated temperature during hot extrusion. The peak intensity of Al_2Ca gradually increases with increases

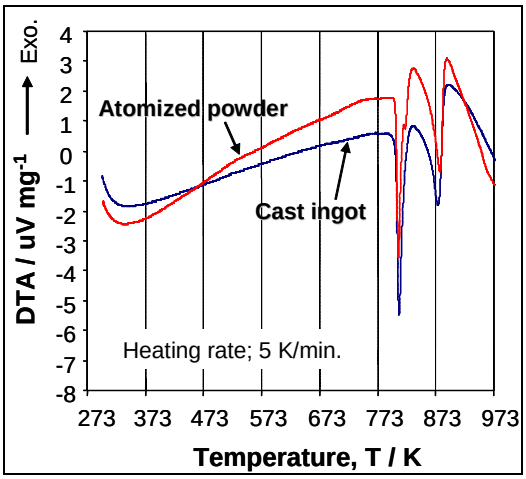

Figure 3. Differential thermal analysis profiles of AMX602 cast ingot billet and as-received coarse SWAP powder.

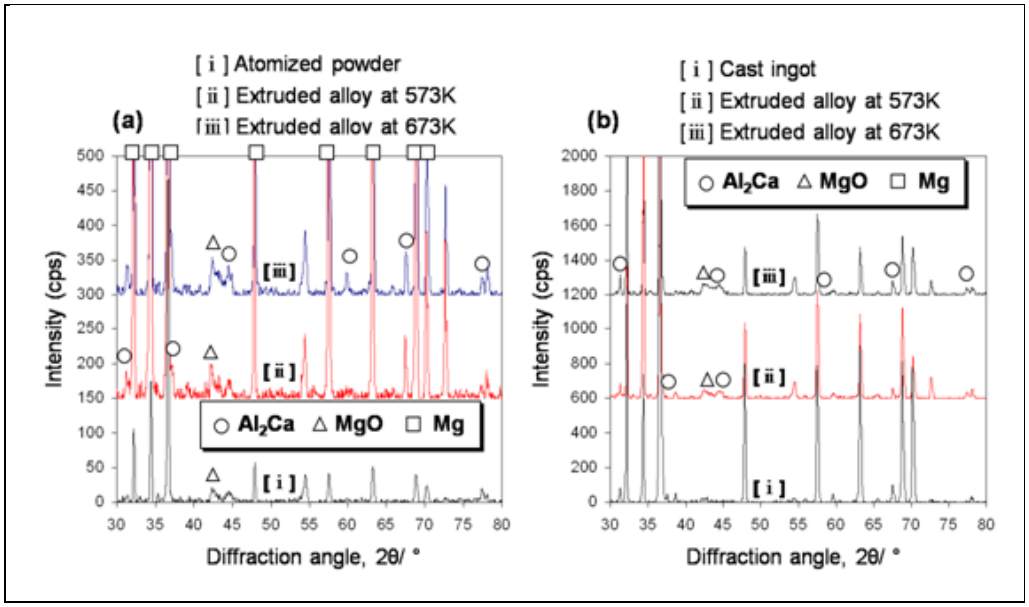

Figure 4. X-ray diffraction patterns of input raw material and AXM602 alloys extruded at 573 and 673 K, using SWAP powder compact (a) and cast ingot billet (b).

in the extrusion temperature. That is, the amount of precipitated Al_2Ca intermetallics increases by a longer thermal history in preheating. On the other hand, the cast ingot material before extrusion contains coarse Al_2Ca intermetallics crystallized during casting (*21*), as shown in figure 4b. There is no remarkable difference in the profile of the wrought alloys extruded at 573–673 K.

Figure 5 shows SEM observation results on the extruded AMX602 alloys using the powder compact (figures 5a-1 and 5a-2) and cast ingot billet (figures 5b-1 and 5b-2). The extrusion temperatures are 573 and 673 K. The powder extruded materials show extremely fine grains 0.3–1.1 μm in diameter compared to the cast ingot extruded ones shown in figures 5b-1 and 5b-2. Regarding the effect of the extrusion temperature on the grain size of the powder extruded material, the mean grain size of the wrought alloy at 573 K, calculated by the image scanning software, is 0.45 μm, and the extruded alloy at 673 K is 0.8 μm. The longer thermal history during preheating in the latter at 673 K causes a small grain growth after dynamic recrystallization in hot extrusion (*22*). The amount of precipitated Al_2Ca intermetallic compounds, which corresponds to fine white particles 100–300 nm distributed in the matrix, is larger for the extruded alloy at 673 K than that of the wrought alloy at 573 K.

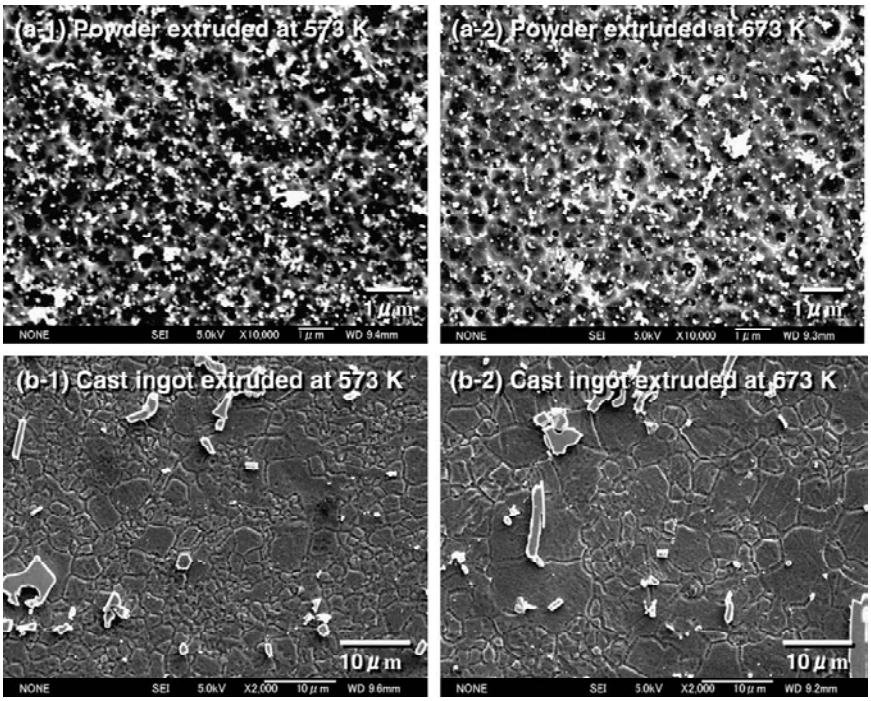

Figure 5. Scanning electron microscope observation of AMX602 alloys extruded at 573 and 673 K, using SWAP powder compact (a-1 and a-2) and cast ingot billet (b-1 and b-2).

On the other hand, figure 5b-1 indicates that the AMX602 wrought alloy extruded at 573 K using the cast ingot billet consists of fine α-Mg grains 1–3 μm in diameter via dynamic recrystallization. Some large grains 5–10 μm in diameter are observed in the matrix. The mean grain size of the extruded materials at 573 K is 1.96 μm. However, when employing the higher preheating temperature at 673 K, many coarse grains over 10 μm exist in the matrix, as shown in figure 5b-2, and a few fine grains <3 μm in diameter are observed. The mean grain size is 3.29 μm.

Compared to the microstructure shown in figure 5b-1, the grain growth and coarsening of figure 5b-2 occurred during extrusion at the higher temperature of 673 K after dynamic recrystallization. Both wrought alloys using cast ingots contain coarse intermetallic compounds with irregular morphologies. Compared to AMX602 cast ingot material, some small compounds are observed because the severe plastic deformation during hot extrusion caused the fragmentation of coarse and brittle intermetallics distributed in the matrix.

As shown in figure 6, SEM-EDS analysis results on the specimen extruded at 573 K, shown in figure 5b-1, indicate the intermetallic dispersoids are mainly Al_2Ca compounds and exist at grain boundaries. A very few small compounds with spherical shapes correspond to Al-Mn intermetallics. Both intermetallics are typical of the conventional AMX602 cast ingot (*17*, *21*).

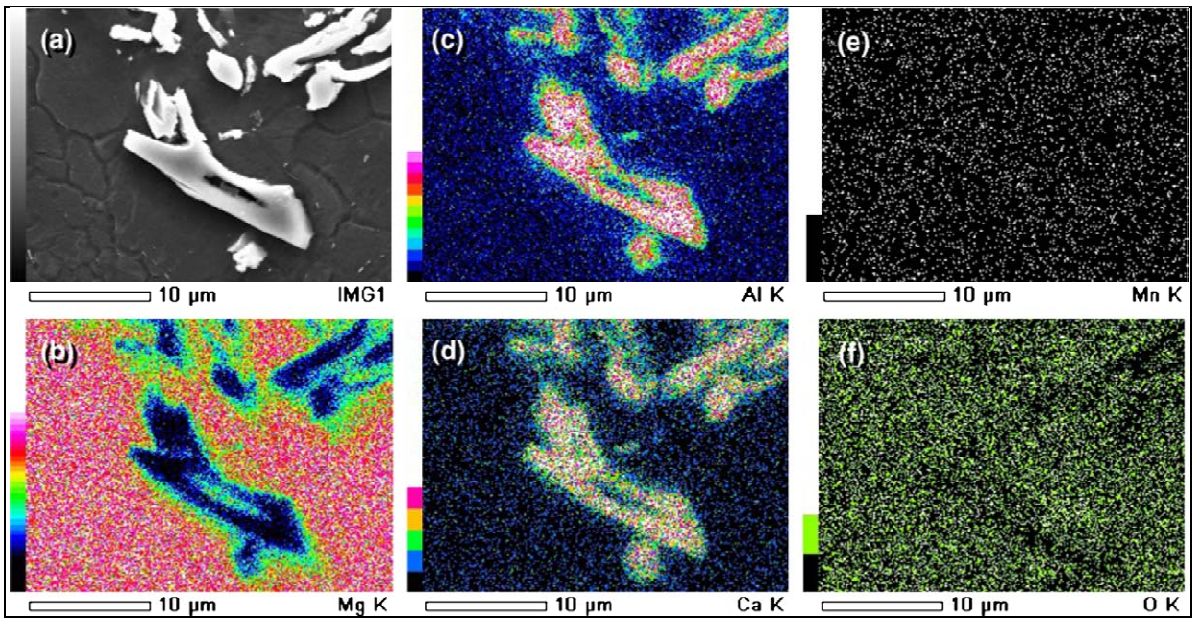

Figure 6. SEM-EDS analysis on intermetallic compounds of AMX602 alloy extruded at 573 K using cast ingot billet (a–f).

Figure 7 shows a microhardness dependence on the grain size of the extruded AMX602 alloys fabricated by using SWAP powder compacts and cast ingot billets. Micro-Vicker's hardness of each material shown in figure 5 is as follows: 113 Hv (figure 5a-1), 94.3 Hv (figure 5a-2), 77.0 Hv (figure 5b-1), and 69.9 Hv (figure 5b-2). The hardness of wrought alloys using atomized powder compacts is higher than that using the cast ingot. This is due to the extremely fine grains and very small intermetallic compounds of the materials mentioned in figure 5. It reveals that the microhardness is proportional to α-Mg grain size, $d^{-0.5}$, and the Hall-Petch relationship is shown in these data.

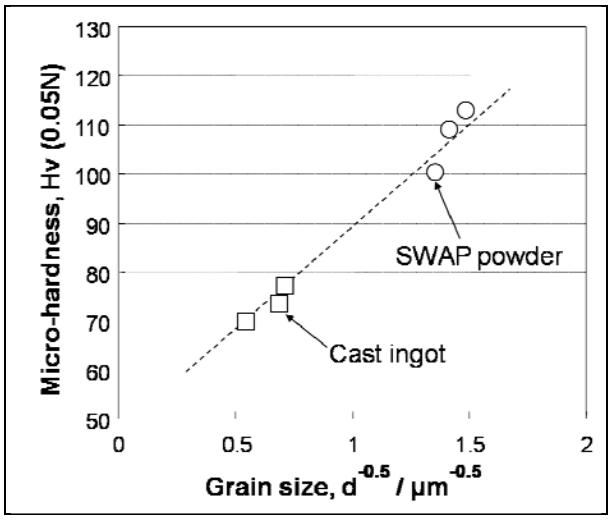

Figure 7. Dependence of micro-Vicker's hardness on grain size of extruded AMX602 alloys.

Figure 8 indicates a dependence of ultimate tensile strength (UTS) and yield tensile strength (YTS) of the extruded AMX602 alloys on the preheating temperature. UTS and YTS of the wrought alloys using the cast ingot billets were 298–311 and 204–251 MPa, respectively. It is reported that the addition of Ca in AM60 alloys is effective not only for its noncombustive properties but also its mechanical properties because coarse intermetallics of Al_2Ca with irregular shapes', as shown in figures 5b-1 and 5b-2, cause the decrease of the tensile properties (*17*, *22*). Therefore, when using the cast ingot billet, the maximum content of Ca is 2% by mass. On the other hand, the alloys using the SWAP powder compacts show an extremely high strength of 391–452 MPa UTS and 358–428 MPa YTS. This is due to the very fine α-Mg grains and Al_2Ca intermetallics shown in figures 5a-1 and 5a-2. In particular, small Al_2Ca precipitated compounds formed by rapid solidification are significantly useful for the dispersion strengthening effect of these magnesium alloys. Concerning their dependence on the temperature, both materials reveal the decrease of UTS and YTS with increase in the preheating temperature due to the grain growth and coarsening, as shown in figure 5. In particular, the decrement of the strength of SWAP powder extruded alloys is larger than that of cast ingot extruded materials. The fine microstructures via dynamic recrystallization of the former are very sensitive to the temperature (*23*), and the grain growth by solid diffusion easily occurs when a higher preheating temperature is applied.

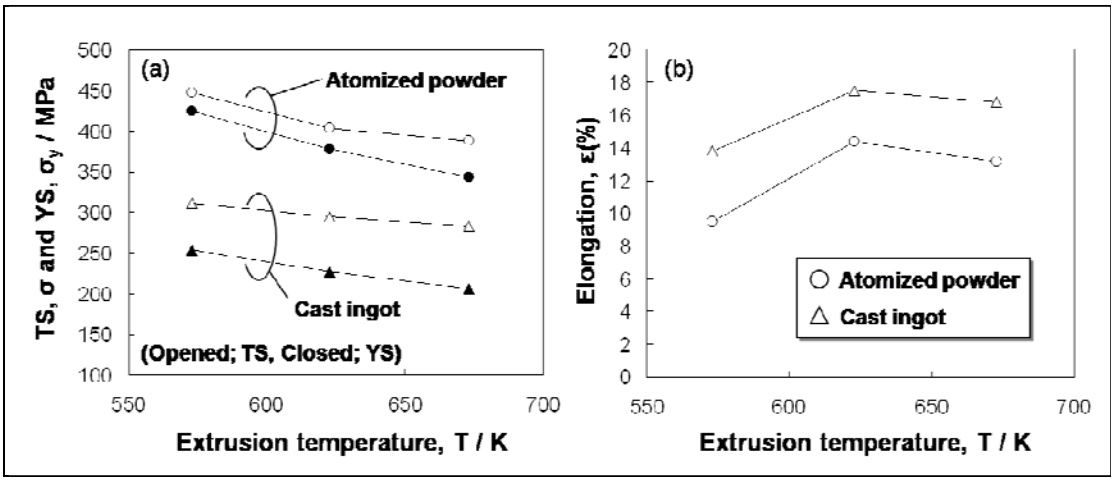

Figure 8. Tensile strength, yield stress, and elongation dependence on preheating temperature.

As shown in figure 8b, the elongation increases with increasing temperature. The SWAP powder extruded alloy at 623 K shows a good balance of 422 MPa UTS and 14.2% elongation. As shown in figure 9a, fine dimpled fracture patterns, which mean typical fractures inside α-Mg grains, are observed, with no fracture at the primary particle boundaries in evidence by SEM observation. The fragmentation of intermetallic compounds at the fractured surface is not observed. Therefore, this material shows a high strength and good ductility. On the other hand, figure 9b indicates the fractured surface of the cast ingot extruded alloy at 623 K. It also shows dimpled fractured patterns. However, the coarse brittle intermetallic compounds include some cracks marked with white arrows, and they correspond to the initiation and propagation of the fracture.

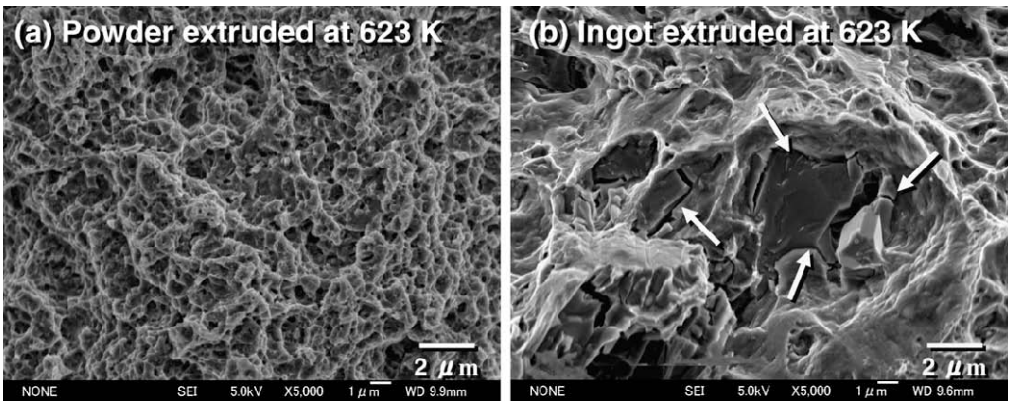

Figure 9. SEM observation on fractured surface of tensile test specimen extruded at 623 K using powder compact (a) and cast ingot (b).

4. Conclusions

The noncombustive AMX602 magnesium alloys were fabricated by extruding the green compacts of rapidly solidified coarse powders 1–4 mm long via SWAP. They showed extremely fine α-Mg grains 0.3–1.1 μm in diameter via dynamic recrystallization. Fine Al_2Ca compounds with a particles size of 100–300 nm were precipitated during hot extrusion and uniformly distributed in the matrix. Compared to the AMX602 extruded alloys using the cast ingot billets, TS and YS of the powder extruded materials showed a significant increase of 30%–45%. The optimization of the preheating temperature before hot extrusion was effective to form very fine recrystallized α-Mg grains and intermetallic dispersoids. For example, a good balance of 422 MPa TS and 14.2% elongation was obtained when employing the preheating temperature at 623 K.

5. References

1. Mordike, B. L.; Ebert, T. Magnesium Properties-Applications-Potential. *Mat. Sci. Eng. A* **2001**, *302*, 37–45.

2. Petch, N. J. The Cleavage Strength of Polycrystals. *J. Iron and Steel Institute* **1953**, *174*, 25–28.

3. Andersson, P.; Caceres, C. H.; Koike, J. Hall-Petch Parameters for Tension and Compression in Cast Mg. *Mater. Sci. Forum* **2003**, *419–422*, 123–128.

4. Chen, Y.; Wang, Q.; Peng, J.; Zhai, C.; Ding, W. Effects of Extrusion Ratio on the Microstructure and Mechanical Properties of AZ31 Mg Alloy. *J. Mater. Process. Tech.* **2007**, *182*, 281–285.

5. Iwahashi, Y.; Wang, J. T.; Horita, Z.; Langdon, T. G. Principle of Equal-Channel Angular Pressing for the Processing of Ultra-Fine Grained Materials. *Scripta Mater.* **1996**, *35*, 143–146.

6. Saito, Y.; Tsuji, N.; Utsunomiya, H.; Sakai, T.; Hong, R. G. Ultra-Fine Grained Bulk Aluminum Produced by Accumulative Roll-Bonding (ARB) Process. *Scripta Mater.* **1998**, *39* (9), 1221–1227.

7. Kondoh, K.; Aizawa, T. Environmentally Benign Fabricating Process of Magnesium Alloy by Cyclical Plastic Working in Solid-State. *Mater. Trans.* **2003**, *44*, 1276–1283.

8. Kondoh, K.; Kawabata, K.; Oginuma, H. Mechanical Properties and Texture of Hot Extruded Magnesium Alloys via RCP Process in Using Coarse Raw Powder Magnesium Technology. *TMS* **2007**, 433–436.

9. Perez-Prado, M. T.; del Valle, J. A.; Ruano, O. A. Grain refinement of Mg–Al–Zn Alloys via Accumulative Roll Bonding. *Scripta Mater.* **2004**, *51*, 1093–1097.

10. Kusy, M.; Grgac, P.; Behulova, M.; Vyrostkova, A.; Miglierini, M. Morphological Variants of Carbides of Solidification Origin in the Rapidly Solidified Powder Particles of Hypereutectic Iron Alloy. *Mat. Sci. Eng. A* **2004**, *375–377*, 599–603.

11. Rawers, J.; Sauer, W.; German, R. Planar Solidification of Rapidly Solidified Powders. *J. Mater. Sci. Lett.* **1993**, *16*, 1327–1329.

12. Wright, R. N.; Anderson, I. E. Age-Hardening Behavior of Dynamically Consolidated Rapidly Solidified Cu-2%Zr Powder. *Mat. Sci. Eng. A* **1989**, *114*, 167–172.

13. Kawamura, Y.; Hayashi, K.; Inoue, A.; Masumoto, T. Rapidly Solidified Powder Metallurgy Mg97Zn1Y2 Alloys With Excellent Tensile Yield Strength Above 600 MPa. *Mater. Trans.* **2001**, *42*, 1172–1176.

14. Kato, H.; Yubuta, K.; Louzguine, D. V.; Inoue, A.; Kim, H. S. Influence of Nanoprecipitation on Strength of Cu60Zr30Ti10 Glass Containing μm-ZrC Particle Reinforcements. *Scripta Mater.* **2004**, *51*, 577–581.

15. Noh, S. J.; Jung, T. K.; Lee, D. S.; Kim, M. S. Microstructure and Compressive Behavior of Al-Base Amorphous/Nanocrystalline Alloys Fabricated by Powder Forging. *Mat. Sci. Eng. A* **2007**, *449–451*, 799–803.

16. Kim, T. S.; Lee, J. K.; Kim, H. J.; Bae, J. C. Consolidation of Cu54Ni6Zr22Ti18 Bulk Amorphous Alloy Powders. *Mat. Sci. Eng. A* **2005**, *402*, 228–233.

17. Sakamoto, M.; Akiyama, S.; Hagio, T.; Ogi, K. Control of Oxidation Surface Film and Suppression of Ignition of Molten Mg-Ca Alloy by Ca Addition. *J. Japan Foundry Engineering Society* **1997**, *69*, 227–233.

18. Nishida, S.; Motomura, I. Estimation of Heat Transfer Coefficient and Temperature Transition on Melt Drag Process of AZ31 Magnesium Alloy by Heat Transfer and Solidification Analysis. *J. Japan Institute of Light Metals* **2008**, *58*, 439–442.

19. Wei, L. Y.; Dunlop, G. L. The Solidification Behavior of Mg-Al-Rare Earth Alloys. *J. Alloy. Compd.* **1996**, *232*, 264–268.

20. Šplíchal, K.; Jurkech, L. Comparison of Oxidation of Cast and Sintered Magnesium Materials in CO2. *J. Nucl. Mater.* **1973**, *48*, 277–286.

21. Anyanwu, I. A.; Gokan, Y.; Suzuki, A.; Kamado, S.; Kojima, Y.; Takeda, S.; Ishida, T. Effect of Substituting Cerium-Rich Mischmetal With Lanthanum on High Temperature Properties of Die-Cast Mg–Zn–Al–Ca–RE Alloys. *Mat. Sci. Eng. A* **2004**, *380*, 93–99.

22. Chandrasekaran, M.; John, Y. M. S. Effect of Materials and Temperature on the Forward Extrusion of Magnesium Alloys. *Mat. Sci. Eng. A* **2004**, *381*, 308–319.

23. Zhang, J. H.; Liu, H. F.; Sun, W.; Lu, H. Y.; Tang, D. X.; Meng, J. Influence of Structure and Ionic Radius on Solubility Limit in the Mg–Re Systems. *Mater. Sci. Forum* **2007**, *561–565*, 143–146.

NO. OF
COPIES ORGANIZATION

1 (PDF only) DEFENSE TECHNICAL INFORMATION CTR
DTIC OCA
8725 JOHN J KINGMAN RD
STE 0944
FORT BELVOIR VA 22060-6218

1 DIRECTOR
US ARMY RESEARCH LAB
IMNE ALC HRR
2800 POWDER MILL RD
ADELPHI MD 20783-1197

1 DIRECTOR
US ARMY RESEARCH LAB
RDRL CIM L
2800 POWDER MILL RD
ADELPHI MD 20783-1197

1 DIRECTOR
US ARMY RESEARCH LAB
RDRL CIM P
2800 POWDER MILL RD
ADELPHI MD 20783-1197

1 DIRECTOR
US ARMY RESEARCH LAB
RDRL D
2800 POWDER MILL RD
ADELPHI MD 20783-1197

ABERDEEN PROVING GROUND

1 DIR USARL
RDRL CIM G (BLDG 4600)

NO. OF COPIES ORGANIZATION

3 CDR US ARMY TACOM
AMSTA TR S
T FURMANIAK
L FRANKS
D TEMPLETON
MS 263
WARREN MI 48397-5000

1 CDR US ARMY TACOM
AMSTA TR R
D HANSEN
WARREN MI 48397-5000

1 PM
SFAE GCSS HBCTS
J ROWE
MS 325
WARREN MI 48397-5000

2 NATL GROUND INTLLGNC CTR
J CRIDER
W GSTATTENBAUER
2055 BOULDERS RD
CHARLOTTESVILLE VA 22091-5391

1 CRUSADER OPM
SFAE GCSS CR E
B ROOPCHAND
BLDG 171A
PICATINNY ARSENAL NJ 07806-5000

2 DARPA
DEFENSE SCIENCE OFC
J GOLDWASSER
S WAX
3701 N FAIRFAX DR
ARLINGTON VA 22203-1714

1 PM BFVS
ATTN SFAE GCSS W BV S
M KING
WARREN MI 48397-5000

1 NVL SURFC WARFARE CTR
CARDEROCK DIV
R PETERSON CODE 28
9500 MACARTHUR BLVD
WEST BETHESDA MD 20817-5700

1 AIR FORCE ARMAMENT LAB
AFATL DLJW
W COOK
EGLIN AFB FL 32542

NO. OF COPIES ORGANIZATION

1 BRIGGS COMPANY
J BACKOFEN
2668 PETERSBOROUGH ST
HERNDON VA 20171-2443

3 BAE ADVNCD CERAMICS SYS
R PALICKA
G NELSON
B CHEN
1960 WATSON WAY
VISTA CA 92083

3 GDLS
W BURKE MZ436 21 24
G CAMPBELL MZ436 30 44
D DEBUSSCHER MZ436 20 29
38500 MOUND RD
STERLING HTS MI 48310-3200

3 GDLS
J ERIDON MZ436 21 24
W HERMAN MZ435 01 24
S PENTESCU MZ436 21 24
38500 MOUND RD
STERLING HTS MI 48310-3200

4 POULTER LAB
SRI INTRNTL
D CURRAN
R KLOOP
L SEAMAN
D SHOCKEY
333 RAVENSWOOD AVE
MENLO PARK CA 94025

1 BAE SYS SIMULA INC
R WOLFFE
10016 SOUTH 51ST ST
PHOENIX AZ 85044

3 BAE SYSTEMS
GROUND SYS DIV
E BRADY
R JENKINS
K STRITTMATTER
PO BOX 15512
YORK PA 17405-1512

1 PENN STATE UNIV
APPLIED RSRCH LAB
ACOUSTICS PRGM
D SWANSON
504L APPLIED SCI BLDG
UNIVERSITY PK PA 16803

NO. OF COPIES	ORGANIZATION
1	PACIFIC NORTHWEST NATL LAB E NYBERG MSIN P7-82 902 BATTELLE BLVD RICHLAND WA 99352
1	UNIV OF VIRGINIA DEPT OF MTRLS SCI & ENG SCHOOL OF ENG & APPL SCI H WADLEY B214 THORNTON HALL 116 ENGINEERS WAY CHARLOTTESVILLE VA 22903
1	CELLULAR MTRLS INTRNTL INC Y MURTY 2 BOARS HEAD LN CHARLOTTESVILLE VA 22903
1	FORCE PROTECTION INDUST INC V JOYNT 9801 HWY 78 LADSON SC 29456
2	US ARMY RSRCH DEV & ENGRG CTR AMSRD NSC IPD B P CUNNIFF J WARD KANSAS ST NATICK MA 01760-5019
1	THE AIR FORCE RSRCH LAB AFRL/MLLMP T TURNER BLDG 655 RM 115 2230 TENTH ST WRIGHT-PATTERSON AFB OH 45433-7817
1	MISSOURI UNIV OF SCI & TECHLGY R MISHRA B37 MCNUTT HALL ROLLA MO 65409-0340
1	US INFANTRY CTR MTRLS LOG NCO – SCI TECHNLGY ADVISOR SOLDIER DIV S VAKERICS 6731 CONSTITUTION LOOP STE 319 FORT BENNING GA 31905

NO. OF COPIES	ORGANIZATION
3	NATL GROUND INTLLGNC CTR D EPPERLY T SHAVER T WATERBURY 2055 BOULDERS RD CHARLOTTESVILLE VA 22911-8318
3	PROG EXECUTIVE OFC – SOLDIER US ARMY DIR TECH MGMT PROJ MGR - SOLDIER EQUIP K MASTERS C PERRITT J ZHENG 15395 JOHN MARSHALL HWY HAYMARKET VA 20169
1	CERADYNE INC M NORMANDIA 3169 RED HILL AVE COSTA MESA CA 92626
2	FOSTER-MILLER J REIGEL R SYKES 195 BEAR HILL RD WALTHAM MA 02451
1	US ARMY RAPID EQUIPPING FORCE R TURNER 10236 BURBECK RD BLDG 361T FORT BELVOIR VA 22060-5806
2	LETTERKENNY ARMY DEPOT PRODUCTION ENGRNG DIV AMSAM LE MO E S K HERSHEY J FRIDAY 1 OVERCASH AVE CHAMBERSBURG PA 17201-4150
1	SAINT GOBAIN D MCELWEE 9 RENEE CT NORTHGATE COMMONS NEWARK DE 19711
1	DIR US ARMY RSRCH LAB RDRL D V WEISS 2800 POWDER MILL RD ADELPHI MD 20783-1197

NO. OF COPIES ORGANIZATION

1 DIR US ARMY RSRCH LAB
RDRL SF
T BOWER
2800 POWDER MILL RD
ADELPHI MD 20783-1197

1 DIR US ARMY RSRCH LAB
RDRL SE
J PELLEGRINO
2800 POWDER MILL RD
ADELPHI MD 20783-1197

1 DIR US ARMY RSRCH LAB
RDRL SES P
2800 POWDER MILL RD
ADELPHI MD 20783-1197

1 DIR US ARMY RSRCH LAB
RDRL SM
T WEATHERSPOON
2800 POWDER MILL RD
ADELPHI MD 20783-1197

1 DEFBAR SYS LLC
M COOPER
1500 S LOUISE
SALEM MO 65560

1 OFC NVL RSRCH
D SHIFLER
875 N RANDOLPH ST
CODE 332 RM 631
ARLINGTON VA 22203-1995

ABERDEEN PROVING GROUND

1 DIR USA EBCC
SCBRD RT
5183 BLACKHAWK RD
APG EA MD 21010-5424

1 CDR USA SBCCOM
AMSCB CII
5183 BLACKHAWK RD
APG EA MD 21010-5424

1 DIR USAMSAA
AMSRD AMS D
BLDG 392

1 CDR USATEC
STEAC LI LV
E SANDERSON
BLDG 400

NO. OF COPIES ORGANIZATION

1 CDR US ARMY DTC
CSTE DTC TT T
M SIMON
RYAN BLDG

75 DIR USARL
RDRL SL
R COATES
RDRL SLB
R BOWEN
RDRL SLB D
D LOWRY
RDRL SLB E
A DIETRICH
RDRL SLB W
W BRUCHEY
L ROACH
RDRL VTU
S WILKERSON
RDRL WM
L BURTON
B FORCH
S KARNA
J MCCAULEY
P PLOSTINS
J SMITH
W WINNER
RDRL WML
M ZOLTOSKI
RDRL WML E
R ANDERSON
RDRL WML H
T FARRAND
L MAGNESS
S SCHRAML
R SUMMERS
RDRL WMM
J BEATTY
R DOWDING
H MAUPIN
J ZABINSKI
RDRL WMM B
B CHEESEMAN
RDRL WMM D
E CHIN
K CHO
W ROY
R SQUILLACIOTI
S WALSH
RDRL WMM F
R CARTER
J CHINELLA
L KECSKES
S MATHAUDHU

NO. OF
COPIES ORGANIZATION

J MONTGOMERY
D SNOHA
RDRL WMS
T ROSENBERGER
RDRL WMP
P BAKER
B BURNS
S SCHOENFELD
RDRL WMP A
C HUMMER
B RINGERS
RDRL WMP B
C HOPPEL
S BILYK
D CASEM
J CLAYTON
D DANDEKAR
M GREENFIELD
Y HUANG
B LEAVY
B LOVE
M RAFTENBERG
M SCHEIDLER
RDRL WMP C
T BJERKE
K KIMSEY
R MUDD
S SEGLETES
W WALTERS
RDRL WMP D
T HAVEL
D KLEPONIS
H MEYER
J RUNYEON
B SCOTT
K STOFFEL
RDRL WMP E
M BURKINS
W GOOCH
D HACKBARTH
E HORWATH
T JONES (2 CPS)
D LITTLE
D SHOWALTER
RDRL WMP F
N GNIAZDOWSKI
R GUPTA
RDRL WMP G
R BANTON

NO. OF
COPIES ORGANIZATION

5 OSAKA UNIVERSITY
JOINING & WELDING RSCH INST
K KONDOH
11-1 MIHOGAOAKA IBARAKI
OSAKA 567-0047 JAPAN

1 AMERICAN EMBASSY SINGAPORE
E STIERNA
PO BOX ODC FPO AP 96507

5 USA ITC-PAC
J P SINGH
7-23-17 ROPPONGI MINATO-KU
TOKYO JAPAN 106-0032